Cu(II) and Zn(II) Complexes with an *N*- and *O*-Donor Ligand: Structural Characterization, Jahn-Teller Effect and Fluorescence

Hai-Wei Kuai, Xiao-Chun Cheng and Xiao-Hong Zhu

Faculty of Life Science and Chemical Engineering, Huaiyin Institute of Technology, Huaian 223003, China

Reprint requests to Dr. Hai-Wei Kuai. Fax: +86-517-83559044. E-mail: hyitshy@126.com

Z. Naturforsch. **2013**, *68b*, 147 – 154 / DOI: 10.5560/ZNB.2013-2325
Received December 9, 2012

Cu(II) and Zn(II) salts react with 5-(1*H*-benzotriazol-1-ylmethyl)isophthalic acid (H_2L) under hydrothermal conditions to yield two new complexes [Cu(L)(DMF)(H_2O)] (**1**) and [Zn(L)] (**2**) [DMF = *N*,*N*-dimethylformamide], which have been characterized by single-crystal and powder X-ray diffraction, IR, elemental and thermogravimetric analyses. As a result, **1** shows a chain structure, further linked together by hydrogen bonding and π–π interactions to give rise to a 3D supramolecular framework. Complex **2** is a binodal (3,6)-connected 2D **kgd** network with $(4^3)_2(4^6.6^6.8^3)$ topology. The influential factors of synthetic strategies on coordination modes of the ligand and structures of the resulting complexes are embodied in the study. Significantly, **1** has structural features consistent with the Jahn-Teller effect. Furthermore, the fluorescence properties of **2** were preliminarily investigated.

Key words: Cu(II) and Zn(II), Jahn-Teller Effect, Fluorescence Properties

Introduction

Recently, supramolecular coordination chemistry is mainly concerned with the design and assembly of crystalline materials based on metal centers and bridging ligands [1 – 4]. Consequently, the investigation of such inorganic-organic hybrid materials has become the main aim of crystal engineering for their interesting properties and potential applications in magnetism, heterogeneous catalysis, ion-recognition, nonlinear optics, and adsorption [5 – 8]. It is known that the functional properties of complexes closely relate with the nature of the metal centers and bridging ligands, and their architectures. For example, complexes with porous framework architectures may show sorption or catalytic properties [9, 10]. Metal ions possessing unpaired electrons, such as Mn(II), Co(II), Ni(II), and Cu(II) *etc*. could be bridged by ligands to form polynuclear subunits which may mediate magnetic interactions [11, 12]. Moreover, complexes containing metal centers with d^{10} electron configuration, such as Zn(II) and Cd(II), may exhibit luminescence [13, 14]. Therefore, it may be significant to pursue structural diversity by attempting different experimental conditions. Among many complicated factors influencing the formation of complexes, the intrinsic nature of organic ligands has been proven to be decisive [15 – 17].

Among the well-employed organic ligands, *N*- and/or *O*-donors are regarded as excellent building blocks for desirable frameworks [18 – 20]. In our previous research work, a series of *N*- and *O*-donor ligands, such as 3,5-bis(2-pyridylmethyl)aminobenzoate, 3,5-bis(pyridin-4-ylmethyl)aminobenzoate and 5-(pyridin-2-ylmethyl)aminoisophthalate, had been employed to synthesize complexes [21 – 23]. Based on these studies, we have recently focused our attention on the utilization of a semi-rigid ligand, 5-(1*H*-benzotriazol-1-ylmethyl)isophthalic acid (H_2L), to construct coordination polymers with diverse structures. H_2L combines both carboxylate and benzotriazolyl functional groups in a single organic ligand. Rigid carboxylate ligands, such as isophthalate and terephthalate have been well studied in the construction of complexes due to their coordinating capacities, appropriate connectivity, and abundant coordination modes [24, 25]. Benzotriazole and its derivatives may give new insight into the structural evolution in crystal engineering due to their steric hindrance and more poten-

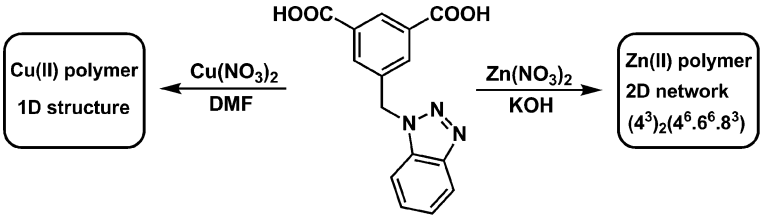

Scheme 1. Simplified representation of the synthesis of **1** and **2**.

tial coordination sites [26]. Therefore, the H_2L ligand may possess an advantage over other *N*- and *O*-donor ligands. Apart from mutable coordination modes of carboxylate, the flexible benzotriazol-1-ylmethyl arm in H_2L has more spatial freedom to adopt different orientations through axial rotation to different angles to satisfy coordinating requirements. The variable coordination modes and conformations of H_2L provide the feasibility to assemble complexes with various structures by regulating synthetic conditions. We report herein the synthesis and characterization of the two new complexes [Cu(L)(DMF)(H_2O)] (**1**) and [Zn(L)] (**2**) [DMF = *N*,*N*-dimethylformamide] (Scheme 1). A Jahn-Teller distortion can be observed in **1**, and the fluorescence of **2** was examined.

Results and Discussion

Preparation

The hydrothermal reaction of $Cu(NO_3)_2{\cdot}3H_2O$ with H_2L at 100 °C in the presence of H_2O-DMF (1 : 1, v/v) as co-solvent yields complex [Cu(L)(DMF)(H_2O)] (**1**). When H_2L reacts with $Zn(NO_3)_2{\cdot}6H_2O$ under hydrothermal conditions in the presence of KOH as alkaline reagent and with the reaction temperature set at 210 °C, the complex [Zn(L)] (**2**) is obtained.

*Structural description of [Cu(L)(DMF)(H_2O)] (**1**)*

The X-ray structure determination has shown that the complex [Cu(L)(DMF)(H_2O)] (**1**) crystallizes in

Table 1. Crystal structure data for **1** and **2**.

	1	**2**
Formula	$C_{18}H_{18}N_4O_6Cu$	$C_{15}H_9N_3O_4Zn$
M_r	449.90	360.62
Crystal size, mm^3	0.30 × 0.30 × 0.06	0.30 × 0.06 × 0.06
Crystal system	triclinic	monoclinic
Space group	$P\bar{1}$	$P2_1/c$
a, Å	9.599(5)	8.347(5)
b, Å	10.082(5)	11.127(5)
c, Å	11.708(5)	16.888(5)
α, deg	85.213(5)	90
β, deg	67.468(5)	119.621(17)
γ, deg	62.681(5)	90
V, Å^3	923.9(8)	1363.5(11)
Z	2	4
D_{calcd}, g cm^{-3}	1.62	1.76
μ(Mo K_α), cm^{-1}	1.2	1.8
F(000), e	462	728
hkl range	±11, ±12, −12 → +14	−10 → +9, −14 → +11, ±22
θ_{max}, deg	1.90–26.00	2.30–28.02
Refl. measd / unique / R_{int}	5099 / 3565 / 0.0118	8303 / 3236 / 0.0744
Param. refined	258	208
$R1$ (F)[a] / $wR2$ (F^2)[b] (all refls.)	0.0453 / 0.1068	0.0468 / 0.1015
GoF (F^2)[c]	1.065	0.973
$\Delta\rho_{fin}$ (max / min), e Å^{-3}	1.00 / −1.79	0.77 / −0.64

[a] $R1 = \Sigma||F_o| - |F_c||/\Sigma|F_o|$; [b] $wR2 = [\Sigma w(F_o^2 - F_c^2)^2/\Sigma w(F_o^2)^2]^{1/2}$, $w = [\sigma^2(F_o^2) + (AP)^2 + BP]^{-1}$, where $P = (\mathrm{Max}(F_o^2, 0) + 2F_c^2)/3$; [c] GoF $= [\Sigma w(F_o^2 - F_c^2)^2/(n_{obs} - n_{param})]^{1/2}$.

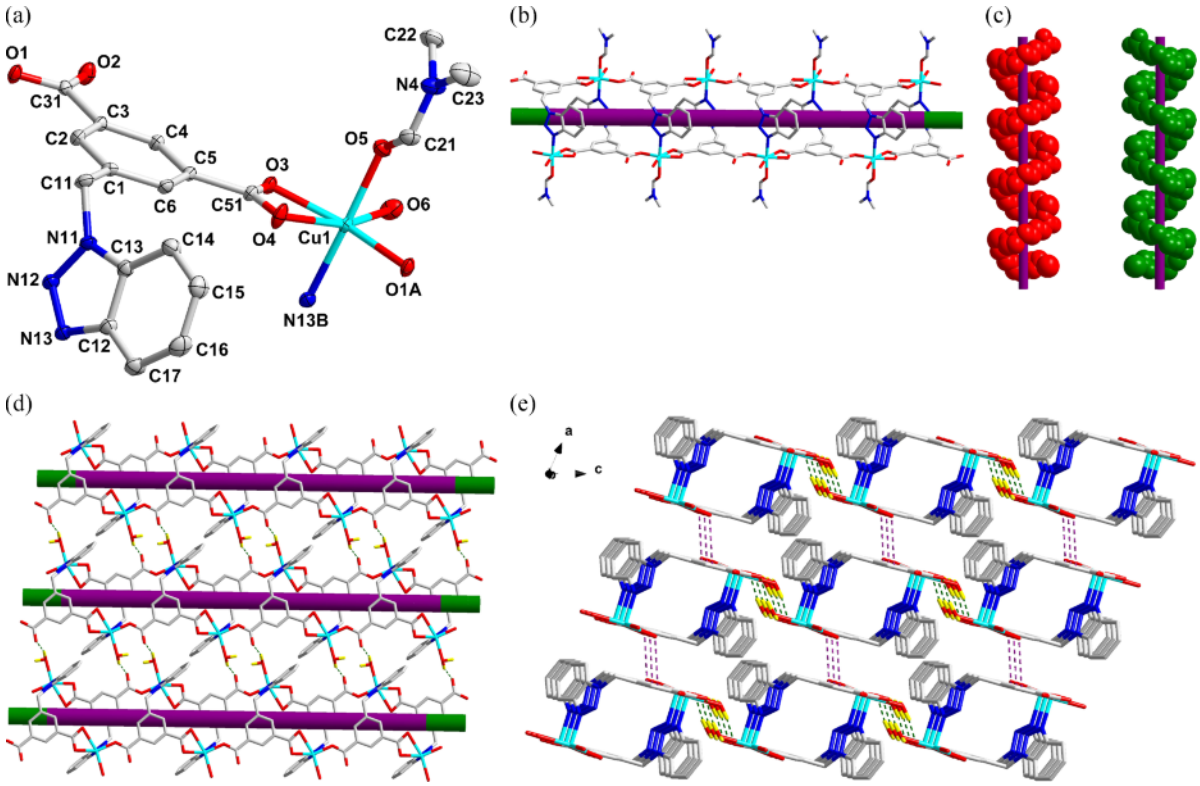

Fig. 1 (color online). (a) The coordination environment of Cu(II) ions in **1** with displacement ellipsoids drawn at the 30% probability level. The hydrogen atoms are omitted for clarity. (b) The neutral double-stranded chain of **1**. (c) Schematic view of the right- and left-handed helical chains in **1**. (d) The 2D network of **1** extended by hydrogen bonding interactions. (e) The 3D framework of **1** constructed through hydrogen bonding and π–π stacking interactions.

the triclinic crystal system with space group $P\bar{1}$ and $Z = 2$ (Table 1). In the solid state it displays a double-stranded chain structure. The H_2L ligand was deprotonated by KOH to the L^{2-} anion. There are one Cu(II), one L^{2-} ligand, one coordinated DMF and one coordinated water molecule in the asymmetric unit of **1**. As shown in Fig. 1a, each Cu(II) is six-coordinated by one benzotriazolyl nitrogen atom, one DMF and one water molecule, and three carboxylate oxygen atoms from two different L^{2-} ligands to furnish a distorted octahedral coordination geometry. The bond lengths and angles around each Cu(II) atom are in the range of 1.935(2) – 2.496(2) Å and 57.65(8)–173.67(9)° (Table 2), respectively. Among the coordination bond lengths, the bonds Cu(1)–O(4) and Cu(1)–O(4) are significantly longer than others, which may be related to a Jahn-Teller distortion (*vide infra*). One of the carboxylate groups in the L^{2-} ligand exhibits μ_1-η^1 : η^0-monodentate coordination mode, and the other is μ_2-η^1 : η^1-chelating (Scheme 2A). As depicted in Fig. 1b, each L^{2-} ligand bridges three Cu(II) centers to give a double-stranded chain structure with the nearest intrachain Cu···Cu distance of 9.043 Å. Interestingly, because of the flex-

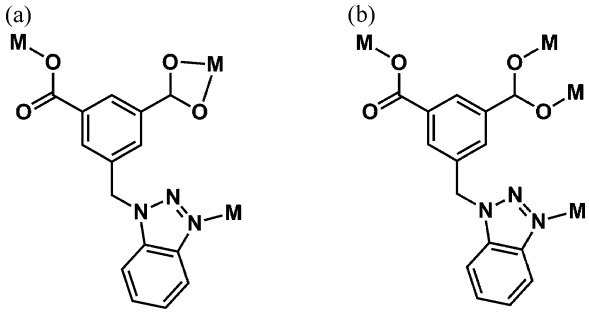

Scheme 2. The coordination modes of the L^{2-} ligand appearing in the complexes.

Table 2. Selected bond lengths (Å) and angles (deg) for complexes **1** and **2**[a].

[Cu(L)(DMF)(H_2O)] (**1**)			
Cu(1)–O(3)	1.982(2)	Cu(1)–O(4)	2.496(2)
Cu(1)–O(5)	1.999(2)	Cu(1)–O(6)	2.306(2)
Cu(1)–O(1)#1	1.935(2)	Cu(1)–N(13)#2	2.046(3)
O(3)–Cu(1)–O(4)	57.65(8)	O(3)–Cu(1)–O(5)	88.80(9)
O(3)–Cu(1)–O(6)	106.55(9)	O(1)#1–Cu(1)–O(3)	154.97(9)
O(3)–Cu(1)–N(13)#2	89.20(9)	O(4)–Cu(1)–O(5)	90.51(9)
O(4)–Cu(1)–O(6)	163.05(8)	O(1)#1–Cu(1)–O(4)	97.32(8)
O(4)–Cu(1)–N(13)#2	93.50(10)	O(5)–Cu(1)–O(6)	82.53(9)
O(1)#1–Cu(1)–O(5)	92.12(9)	O(5)–Cu(1)–N(13)#2	173.67(9)
O(1)#1–Cu(1)–O(6)	98.36(9)	O(6)–Cu(1)–N(13)#2	92.29(9)
O(1)#1–Cu(1)–N(13)#2	92.24(9)		
[Zn(L)] (**2**)			
Zn(1)–O(1)	2.049(2)	Zn(1)–O(4)#1	1.9945(19)
Zn(1)–N(13)#2	2.030(2)	Zn(1)–O(3)#3	1.9774(17)
O(1)–Zn(1)–O(4)#1	127.60(8)	O(1)–Zn(1)–N(13)#2	112.02(10)
O(1)–Zn(1)–O(3)#3	100.00(9)	O(4)#1–Zn(1)–N(13)#2	108.71(9)
O(3)#3–Zn(1)–O(4)#1	105.20(8)	O(3)#3–Zn(1)–N(13)#2	98.45(8)

[a] Symmetry transformations used to generate equivalent atoms: for **1**: #1 x, $1+y$, z; #2 $2-x$, $-y$, $2-z$; for **2**: #1 $-x$, $-1/2+y$, $3/2-z$; #2 $-x$, $2-y$, $1-z$; #3 x, $3/2-y$, $-1/2+z$.

ibility of the L^{2-} ligand, the double-chain extends along the *b* axis direction in a spiral way. If some organic moieties are ignored, a pair of right- and left-handed helical chains can be distinguished in the neutral double-stranded chain (Fig. 1c). Each chain is interlinked to form a supramolecular layer motif *via* hydrogen bonding interactions between water molecules and carboxylate oxygen atoms (Fig. 1d) [O(6)–H(17)···O(2)#1 with O(6)···O(2)#1 = 2.785(4) Å, ∠O(6)–H(17)···O(6)#1 = 162° (#1: 2–*x*, –*y*, 1–*z*)]. Another structural feature in **1** is that the adjacent layers recognize each other through strongly offset π–π stacking interactions, ultimately leading to a 3D supramolecular framework (Fig. 1e). The centroid-centroid distance between the central benzene rings is 3.662 Å.

*Structural description of [Zn(L)] (**2**)*

Complex **2** crystallizes in the monoclinic system with space group $P2_1/c$ and $Z = 4$, exhibiting a 2D network structure based on Zn(II) centers and L^{2-} ligands. There are one Zn(II) atom and one L^{2-} ligand in the asymmetrical unit. In complex **2**, each Zn(II) is four-coordinated by one benzotriazolyl N atom and three carboxylate O atoms from three different L^{2-} ligands to furnish a distorted tetrahedral coordination geometry (Fig. 2a). The bond lengths vary from 1.9774(17) to 2.049(2) Å, and the bond angles are in the range of 98.45(8) to 127.60(8)°. The carboxylate groups in L^{2-} adopt μ_1-$\eta^1:\eta^0$-monodentate and μ_2-$\eta^1:\eta^1$-bridging coordination modes resulting in the formation of carboxylate-bridged binuclear secondary building units (SBU) [$Zn_2(COO)_2$] with a Zn···Zn distance of 3.82 Å, which is shorter than the sum of two van der Waals radii (4.20 Å). In **2**, each L^{2-} ligand links three SBUs while each SBU is surrounded by six L^{2-} ligands. This kind of connection proceeds infinitely to generate a 2D network structure (Fig. 2b). If using topology to analyze the structure, each SBU could be regarded as a 6-connector node and the L^{2-} ligand as a 3-connector node, and thus, the resultant structure of **2** could be simplified as a binodal (3,6)-connected 2D **kgd** network with $(4^3)_2(4^6.6^6.8^3)$ topology (Fig. 2c) [27].

*PXRD and thermal stabilities of complexes **1** and **2***

The phase purities of **1** and **2** could be proven by powder X-ray diffraction (PXRD). As shown in Fig. 3, each PXRD pattern of the as-synthesized sample is consistent with the simulated one.

Thermogravimetric analyses (TGA) were carried out for complexes **1** and **2**, and the results are shown in Fig. 4. For complex **1**, there is a weight loss of 4.3 % from 119 °C to 190 °C corresponding to the release of water (calcd. 4.0 %). A continuous weight loss starting at 206 °C can be assigned to the gradual release of DMF molecules preceding the subsequent decomposition of the framework of **1**. No obvious weight loss can be observed before the decomposition of the frame-

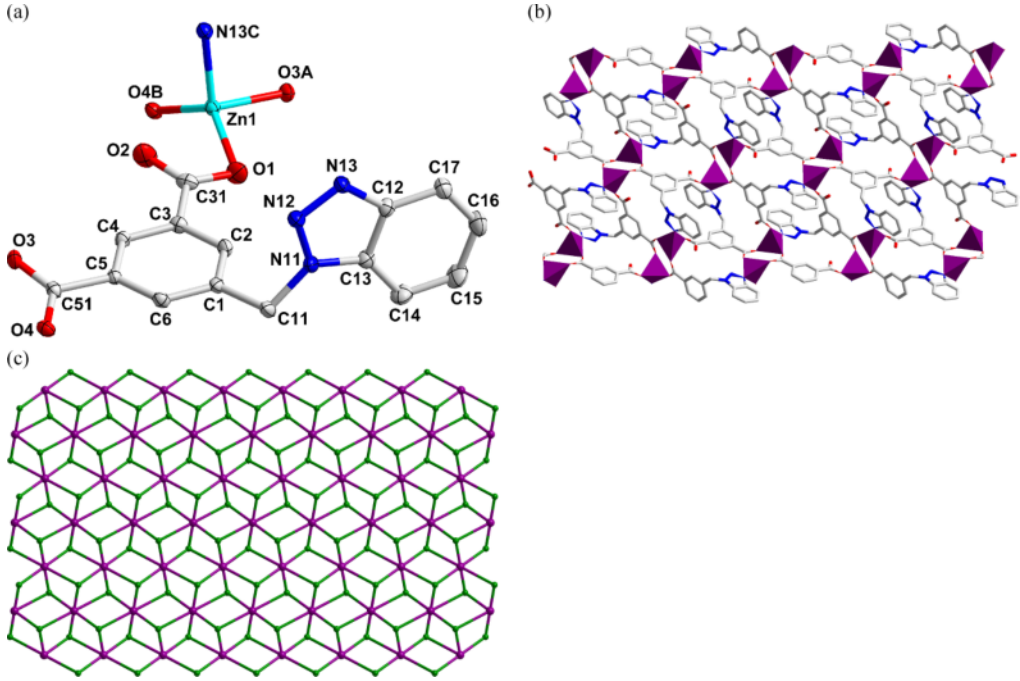

Fig. 2 (color online). (a) The coordination environment of Zn(II) ions in **2** with displacement ellipsoids drawn at the 30% probability level. The hydrogen atoms are omitted for clarity. (b) View of the 2D network of **2**. (c) View of the binodal (3,6)-connected 2D **kgd** network of **2**.

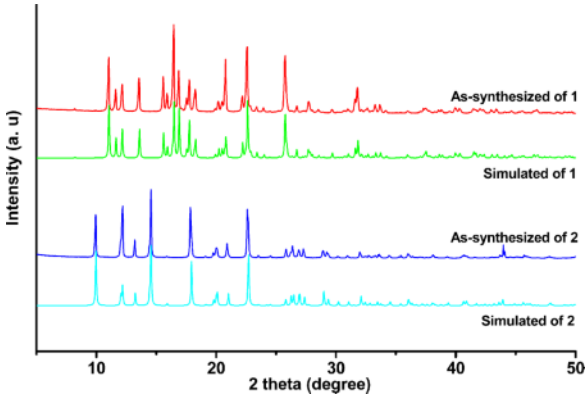

Fig. 3 (color online). The PXRD patterns of complexes **1** and **2**.

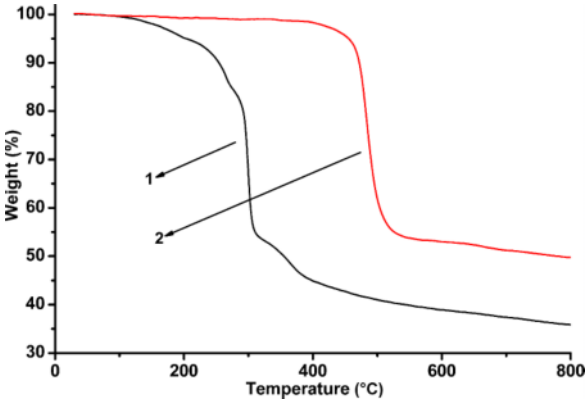

Fig. 4. TGA curves of complexes **1** and **2**.

work at 430 °C for **2**, which further confirms the absence of solvent in its structure.

*Jahn-Teller effect in complex **1***

According to Crystal Field Theory (CFT), six-coordinated Cu(II) in [Cu(L)(DMF)(H_2O)] (**1**) should show octahedral coordination geometry (O_h field) with six equivalent coordinative bonds. As the bond lengths of Cu(1)–O(4) and Cu(1)–O(4) are significantly longer than others (Table 2), the molecular distortion might originate from the Jahn-Teller effect [28, 29]. The two e_g orbitals in the Cu(II) $\{d^9[(t_{2g})^6(e_g)^3]\}$ electron configuration are asymmetrically occupied, and thus complex **1** should have a degenerate electronic ground state [30, 31]. Thereby, the Jahn-Teller distortion may

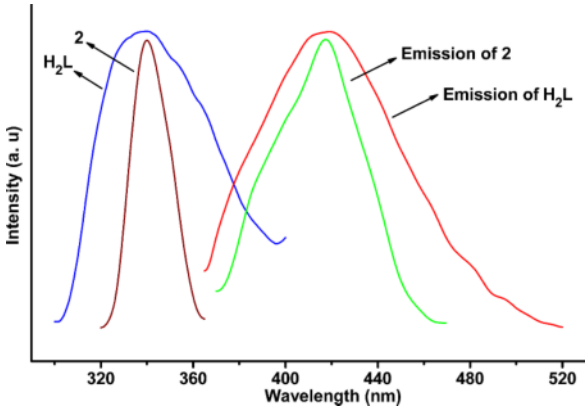

Fig. 5. Fluorescence of **2** and the H_2L ligand in the solid state at room temperature.

take place to lower the overall energy of the complex **1** accounting for the distortion of the octahedral molecular structure [32].

Luminescence properties

The luminescence properties of complexes with d^{10} metal centers such as Zn(II) are of interest for their potential applications as photoactive materials [33 – 35]. Therefore, the luminescence of **2** and of the free H_2L ligand, was investigated in the solid state at room temperature. As shown in Fig. 5, intense bands were observed at 417 nm ($\lambda_{ex} = 339$ nm) for **2** and 418 nm ($\lambda_{ex} = 337$ nm) for the H_2L ligand. As for the source of fluorescence of the complex, it may be assigned to intra-ligand transitions of the coordinated L^{2-} ligands since a similar emission can be observed for the free H_2L ligand [36, 37].

Conclusion

The ligand 5-(1*H*-benzotriazol-1-ylmethyl)isophthalic acid (H_2L) as an organic building block reacts with Cu(II) and Zn(II) salts under different hydrothermal conditions to yield the two complexes [Cu(L)(DMF)(H_2O)] (**1**) and [Zn(L)] (**2**). Complex **1** has a chain structure, further linked by hydrogen bonding and π–π interactions to form a 3D supramolecular framework. Complex **2** is a binodal (3,6)-connected 2D **kgd** network with $(4^3)_2(4^6.6^6.8^3)$ topology. Apart from different crystal structures of **1** and **2**, the coordination modes are also different in these two complexes. The results show influential factors of synthetic strategies: metal salts, solvents, and reaction temperature on coordination modes of a ligand and the structures of the resulting complexes, and illustrate the aesthetic diversity of coordinative supramolecular chemistry. A Jahn-Teller distortion can be observed in complex **1**. As expected, the zinc polymer **2** exhibits strong luminescent emission.

Experimental Section

All commercially available chemicals were of reagent grade and used as received without further purification. The H_2L ligand was synthesized *via* the experimental procedure reported in the literature [38]. Elemental analysis of C, H, and N were taken on a Perkin-Elmer 240C elemental analyzer. Infrared spectra (IR) were recorded on a Bruker Vector22 FT-IR spectrophotometer by using KBr pellets. Thermogravimetric analysis (TGA) was performed on a simultaneous SDT 2960 thermal analyzer under nitrogen atmosphere with a heating rate of 10 °C min^{-1}. Powder X-ray diffraction (PXRD) patterns were measured on a Shimadzu XRD-6000 X-ray diffractometer with Cu K_α ($\lambda = 1.5418$ Å) radiation at room temperature. The luminescence spectra for the powdered solid samples were measured on an Aminco Bowman Series 2 spectrofluorometer with a xenon arc lamp as the light source. In the measurements of emission and excitation spectra the pass width was 5 nm, and all measurements were carried out under the same experimental conditions.

*Preparation of [Cu(L)(DMF)(H_2O)] (**1**)*

The reaction mixture of $Cu(NO_3)_2 \cdot 3H_2O$ (72.4 mg, 0.3 mmol), H_2L (29.7 mg, 0.1 mmol) and 5 mL DMF in 5 mL H_2O was sealed in a 16 mL Teflon-lined stainless-steel container and heated at 100 °C for 48 hours. Then the oven was cooled at a rate of 10 °C h^{-1}. After cooling to room temperature, aqua-blue plate crystals of **1** were obtained with an approximate yield of 20 % based on H_2L. – $C_{18}H_{18}N_4O_6Cu$ (449.90): calcd. C 48.05, H 4.03, N 12.45; found C 48.26, H 3.88, N 12.16 %. – IR (KBr pellet, cm^{-1}): $\nu = 3425$ (m), 1646 (s), 1618 (s), 1572 (s), 1493 (w), 1457 (m), 1438 (s), 1415 (m), 1364 (s), 1345 (s), 1281 (w), 1239 (m), 1226 (m), 1114 (m), 763 (s), 717 (m), 694 (m).

*Preparation of [Zn(L)] (**2**)*

The reaction mixture of $Zn(NO_3)_2 \cdot 6H_2O$ (89.2 mg, 0.3 mmol), H_2L (29.7 mg, 0.1 mmol) and KOH (11.2 mg, 0.2 mmol) in 10 mL H_2O was sealed in a 16 mL Teflon-lined stainless-steel container and heated at 210 °C for 72 h. Then the oven was shut off and left to cool to ambient temperature. Colorless slender crystals of **2** were obtained with an

approximate yield of 20% based on H_2L. – $C_{15}H_9N_3O_4Zn$ (360.62): calcd. C 49.95, H 2.52, N 11.65; found C 49.66, H 2.75, N 11.53%. – IR (KBr pellet, cm^{-1}): $\nu = 1627$ (s), 1573 (s), 1494 (w), 1456 (s), 1433 (w), 1383 (s), 1357 (s), 1289 (m), 1225 (m), 1192 (w), 1149 (w), 807 (w), 766 (s), 743 (s), 724 (s).

X-Ray structure determinations

The crystallographic data collections for complexes **1** and **2** were carried out on a Bruker Smart Apex CCD area detector diffractometer using graphite-monochromatized Mo K_α radiation ($\lambda = 0.71073$ Å) at 293(2) K. The diffraction data were integrated by using the program SAINT [39], which was also used for the intensity corrections for Lorentz and polarization effects. Semi-empirical absorption corrections were applied using the program SADABS [40]. The structures of **1** and **2** were solved by Direct Methods, and all non-hydrogen atoms were refined anisotropically on F^2 by full-matrix least-squares techniques using the SHELXS/L-97 crystallographic software package [41–43]. In **1** and **2**, all hydrogen atoms at C atoms were generated geometrically, the hydrogen atoms at the water molecule in **1** could be found at a reasonable position in the difference Fourier maps and located there. The crystal parameters and details of data collection and refinement are summarized in Table 1. Selected bond lengths and angles are listed in Table 2.

CCDC 914153 and 914154 contain the supplementary crystallographic data for this paper. These data can be obtained free of charge from The Cambridge Crystallographic Data Centre *via* www.ccdc.cam.ac.uk/data_request/cif.

Acknowledgement

The authors gratefully acknowledge Huaian Administration of Science & Technology of Jiangsu Province of China (HAG2012022) for financial support of this work.

[1] Y. Z. Zheng, M. L. Tong, W. Xue, W. X. Zhang, X. M. Chen, F. Grandjean, G. J. Long, *Angew. Chem. Int. Ed.* **2010**, *46*, 6076–6080.
[2] T. Uemura, Y. Ono, Y. Hijikata, S. Kitagawa, *J. Am. Chem. Soc.* **2010**, *132*, 4917–4924.
[3] C. Y. Chen, J. Peng, Y. Shen, D. Chen, H. Q. Zhang, C. L. Meng, *Z. Naturforsch.* **2011**, *66b*, 43–48.
[4] G. C. Liu, J. X. Zhang, X. L. Wang, H. Y. Lin, A. X. Tian, Y. F. Wang, *Z. Naturforsch.* **2011**, *66b*, 125–132.
[5] Y. Kobayashi, B. Jacobs, M. D. Allendorf, J. R. Long, *Chem. Mater.* **2010**, *22*, 4120–4122.
[6] S. Hasegawa, S. Horike, R. Matsuda, S. Furukawa, K. Mochizuki, Y. Kinoshita, S. Kitagawa, *J. Am. Chem. Soc.* **2007**, *129*, 2607–2614.
[7] J. F. Kou, M. Su, Y. H. Zhang, Z. D. Huang, S. W. Ng, G. Yang, *Z. Naturforsch.* **2010**, *65b*, 1467–1471.
[8] C. Kallfaß, C. Hoch, H. Schier, A. Simon, H. Schubert, *Z. Naturforsch.* **2010**, *65b*, 1427–1433.
[9] J. R. Li, R. J. Kuppler, H. C. Zhou, *Chem. Soc. Rev.* **2009**, *38*, 1477–1504.
[10] J. S. Seo, D. Whang, H. Lee, S. I. Jun, J. Oh, Y. J. Jeon, K. Kim, *Nature* **2000**, *404*, 982–986.
[11] J. Milon, M. C. Daniel, A. Kaiba, P. Guionneau, S. Brandès, J. P. Sutter, *J. Am. Chem. Soc.* **2007**, *129*, 13872–13878.
[12] K. R. Dunbar, *Angew. Chem., Int. Ed. Engl.* **1996**, *35*, 1659–1661.
[13] B. Zhao, X. Y. Chen, P. Cheng, D. Z. Liao, S. P. Yan, Z. H. Jiang, *J. Am. Chem. Soc.* **2004**, *126*, 15394–15395.
[14] X. Feng, Y. H. Wen, Y. Z. Lan, Y. L. Feng, C. Y. Pan, Y. G. Yao, *Inorg. Chem. Commun.* **2009**, *12*, 89–91.
[15] G. Z. Liu, S. H. Li, L. Y. Wang, *CrystEngComm* **2012**, *14*, 880–889.
[16] G. X. Liu, Y. Q. Huang, Q. Chu, T. A. Okamura, W. Y. Sun, H. Liang, N. Ueyama, *Cryst. Growth Des.* **2008**, *8*, 3233–3245.
[17] R. Cao, D. Sun, Y. Liang, M. Hong, K. Tatsumi, Q. Shi, *Inorg.Chem.* **2002**, *41*, 2087–2094.
[18] S. S. Chen, M. Chen, S. Takamizawa, M. S. Chen, Z. Su, W. Y. Sun, *Chem. Commun.* **2011**, *47*, 752–754.
[19] S. S. Chen, M. Chen, S. Takamizawa, P. Wang, G. C. Lv, W. Y. Sun, *Chem. Commun.* **2011**, *47*, 4902–4904.
[20] Z. Su, M. Chen, T. Okamura, M. S. Chen, S. S. Chen, W. Y. Sun, *Inorg. Chem.* **2011**, *50*, 985–991.
[21] H. W. Kuai, X. C. Cheng, X. H. Zhu, *J. Coord. Chem.* **2011**, *64*, 1636–1644.
[22] H. W. Kuai, X. C. Cheng, X. H. Zhu, *J. Coord. Chem.* **2011**, *64*, 3323–3332.
[23] H. W. Kuai, X. C. Cheng, L. D. Feng, X. H. Zhu, *Z. Anorg. Allg. Chem.* **2011**, *637*, 1560–1565.
[24] Z. Su, J. Fan, M. Chen, T. A. Okamura, W. Y. Sun, *Cryst. Growth Des.* **2011**, *11*, 1159–1169.
[25] Z. Su, S. S. Chen, J. Fan, M. S. Chen, Y. Zhao, W. Y. Sun, *Cryst. Growth Des.* **2010**, *10*, 3675–3684.
[26] G. E. Kostakis, P. Xydias, E. Nordlander, J. C. Plakatouras, *Inorg. Chim. Acta* **2012**, *383*, 327–331.
[27] V. A. Blatov, *IUCr CompComm Newsletter* **2006**, *7*, 4–38.

[28] H. Aghabozorg, G. J. Palenik, R. C. Stoufer, J. Summers, *Inorg. Chem.* **1982**, *21*, 3903 – 3907.
[29] C. J. Simmons, A. Clearfield, W. Fitzgerald, S. Tyagi, B. J. Hathaway, *Inorg. Chem.* **1983**, *22*, 2463 – 2466.
[30] A. Avdeef, J. A. Costamagna, J. P. Fackler, Jr., *Inorg. Chem.* **1974**, *8*, 1854 – 1863.
[31] J. P. Fackler, A. Avdeef, *Inorg. Chem.* **1974**, *8*, 1864 – 1875.
[32] R. S. Gall, N. G. Connelly, L. F. Dahl, *J. Am. Chem. Soc.* **1974**, *12*, 4017 – 4019.
[33] Y. B. Dong, P. Wang, R. Q. Huang, M. D. Smith, *Inorg. Chem.* **2004**, *43*, 4727 – 4739.
[34] D. M. Ciurtin, N. G. Pschirer, M. D. Smith, U. H. F. Bunz, H.-C. zur Loye, *Chem. Mater.* **2001**, *13*, 2743 – 2745.
[35] H. W. Kuai, X. C. Cheng, X. H. Zhu, *Inorg. Chem. Commun.* **2012**, *25*, 43 – 47.
[36] B. Valeur, *Molecular Fluorescence: Principles and Applications*, Wiley-VCH, Weinheim, **2002**.
[37] Y. Q. Huang, B. Ding, H. B. Song, B. Zhao, P. Ren, P. Cheng, H. G. Wang, D. Z. Liao, S. P. Yan, *Chem. Commun.* **2006**, 4906 – 4908.
[38] J. Fan, B. E. Hanson, *Inorg. Chem.* **2005**, *44*, 6998 – 7008.
[39] SAINT, Program for Data Extraction and Reduction, Bruker Analytical X-ray Instruments Inc., Madison, Wisconsin (USA) **2001**.
[40] G. M. Sheldrick, SADABS, Program for Empirical Absorption Correction of Area Detector Data, University of Göttingen, Göttingen (Germany) **1997**.
[41] G. M. Sheldrick, SHELXS/L-97, Programs for Crystal Structure Determination, University of Göttingen, Göttingen (Germany) **1997**.
[42] G. M. Sheldrick, *Acta Crystallogr.* **1990**, *A46*, 467 – 473.
[43] G. M. Sheldrick, *Acta Crystallogr.* **2008**, *A64*, 112 – 122.